Surface Technology White Papers
98 (3), 1-10 (June 2011)

Corrosion Resistance Mechanism of a Chromium-Free Zinc-Flake Coating Film on Scratched Areas

by
*Masayuki Iijima and Masayuki Tsujimoto**
Yuken Industry Co., Ltd.,
Kariya City, Aichi Prefecture, Japan

ABSTRACT

Chromium-free zinc flake coatings (zinc-rich paint) are used for automotive parts and construction parts, etc. that require a high degree of corrosion protection. The demand for this process is extremely high due in part to its being an environmentally-friendly, chromium-free process. Currently, the automotive industry and others are looking for this type of coating which exhibits superior performance. In 2008, we studied the high corrosion resistance mechanism of the chromium-free zinc flake coating film using polarization curves. Currently, we are working on studying this mechanism in greater detail, focusing on how corrosion is controlled, even on areas that are scratched.

Keywords: Zinc-flake coatings, zinc-rich paint, chromium-free coatings, corrosion resistance

Introduction

Steel is a metal widely used in the automotive and construction sectors, among others. As it very easily corrodes, steel is generally processed with a corrosion protection treatment. In particular, when small parts and fasteners are processed, because of dimensional accuracy requirements, it is difficult to apply a thick film to those parts, as compared to large parts that may be painted or hot-dip galvanized.

Therefore, these small parts are generally required to have thin films applied by electroplating or thin-film coating processes. Zinc plating is often applied to parts used as interior components requiring a good appearance, while a zinc flake coating is normally applied to underbody parts used in the engine area requiring a high corrosion protection performance.

Previously, thin-film zinc flake coatings often contained a chromium compound as a binder component, and it was widely used. However, in keeping with the global trend to reduce environmentally harmful substances, the use of chromium compounds is currently strictly controlled. Therefore, non-chromium zinc flake coatings containing no toxic metals is getting much attention.

In previous work,[1] we focused mainly on (1) the ability to prevent the film from corroding (zinc dissolution) and (2) the performance of different metal couples with zinc/iron for corrosion protection. We studied the corrosion protection mechanism of zinc flake coatings by comparing them with zinc plating using polarization curves. We also emphasized that silica-type zinc flake coatings provide good corrosion protection because it is advantageous in terms of the above two areas.

However, when we consider the mechanism of corrosion protection, the condition of the film surface changes over time, and evaluating the surface condition only at the initial state is insufficient. In scratched areas of a film surface in particular, byproducts created in the corrosion process are considered to have a significant effect on the film's corrosion protection performance. As thin-film zinc flake coating has no chromium and also dip spin technology is widely used with this paint, corrosion protection on scratched areas is a very important factor.

* Corresponding author:
Masayuki "Masa" Tsujimoto
Yuken Industry Co., Ltd.
50 Bawari, Noda,
Kariya City, Aichi Pref. 448-8511 Japan
Phone: +81-566-21-7311
Email: tsujimot@yuken-ind.co.jp

Alternative address:
Yuken America, Inc.
40000 Grand River Avenue, Suite 108
Novi, MI 48375
Phone: 248-888-7771
Fax: 248-888-7757
Email: yuken_america@sbcglobal.net

In this research, we focused on the corrosion protection on scratched areas of the silica-type zinc flake coating surface and studied its mechanism by evaluating the changes occurring in the condition of the surface.

Experimental

Preparation of test samples

In this study, we tested zinc flake coatings with a silica-base topcoat that reacts with and permeates into the basecoat (referred to as the silica-reaction-type hereafter). Cold-rolled steel coupons (JIS-G3141) [0.8 × 50 × 100 mm] were used as test coupons. They were painted with the zinc flake coating using a bar-coater under standard baking/drying conditions (Refer to Table 1 for a summary of the silica-reaction-type zinc flake coating process.). As a reference, we also evaluated coupons processed with two layers of basecoat only.

Table 1 - Summary of a silica reaction type zinc flake coating process.

Basecoat (Two coats)			Topcoat		
Thickness, µm	Main components	Baking condition	Thickness, µm	Main component	Drying condition
8.0 - 10.0	Zn, Al, Si, Ti	260°C×30 min	0.5 - 1.0	Si	100°C×15 min

Corrosion protection evaluation

A cyclic corrosion test (referred to as CCT hereafter) was used as an accelerated test to evaluate the corrosion protection performance. . A Suga Test Instrument CYP-90 was used in this test. One cycle consisted of (1) salt spray (50°C, 17 hr); (2) dry (70°C, 3 hr); (3) salt spray (50°C, 2 hr) and (4) dry (room temperature, 2 hr). The bottom halves of the samples were cross-cut to evaluate the corrosion protection in scratched areas.

Surface condition evaluation

In evaluating corrosion protection, we took samples at every ten CCT cycles, and performed image observations, qualitative/quantitative analysis and mapping analysis using the SEM-EDS. Basic information about the SEM-EDS is as follows.

Tester:	JSM-6480A (JEOL Technics, Ltd.)
Accelerating voltage:	10 kV
Magnification:	200×, 1000×
Spot size:	50 (image observation)
	68~70 (quantitative/qualitative analysis, mapping analysis)

Polarization curve measurements

We used an SEM-EDS to evaluate the surface condition. We also measured the polarization curve of each sample, and evaluated film electrochemical characteristics using a potentiostat (Solartron Group Ltd., 1285A) configured with three electrodes.[2] Each test sample was measured in a 5% NaCl solution of pH 7.0 ± 0.2, as shown in Fig. 1. The counter electrode was made of platinum, and a saturated calomel electrode (SCE) was used as the reference electrode. The potential scanning speed was 1.0 mV/sec.

Results and discussion

Corrosion resistance performance results

Figure 2 shows the CCT results for each test sample. The test coupon with only the basecoat shows red rust in the scratched areas at 40 cycles. On the other hand, the test coupon processed with both the basecoat and topcoat shows no red rust even

after 60 cycles. Using the same evaluation method, a sample processed with yellow hexavalent chromate over zinc plating (thickness, 8 mm) shows red rust at around 8 cycles. Therefore, we can confirm that the silica-reaction-type zinc flake coating provides excellent corrosion protection.

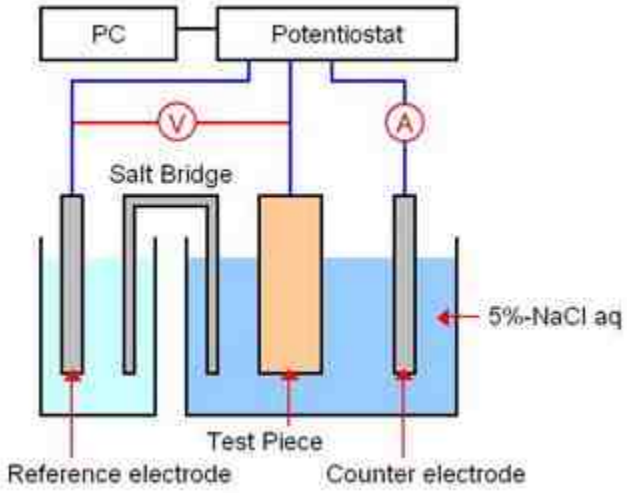

Figure 1 - Polarization curve measurement equipment.

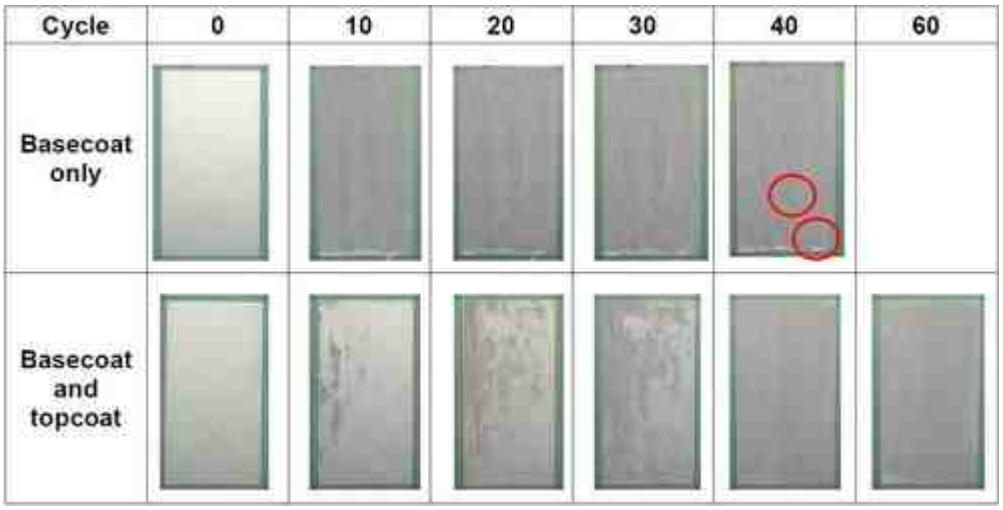

Figure 2 - Cyclic corrosion test results.

SEM surface observations

Figures 3 and 4 show the results of the SEM surface observations. In the basecoat-only sample coupons, a type of corrosion byproduct covered the entire surface after 10 cycles and its particle configuration appeared to change from narrow to wide to narrow as the CCT proceeded from 10 to 20 to 40 cycles. Moreover, the scratched area was covered by the corrosion byproduct at 10 cycles. More corrosion byproduct was observed in the scratched area than in the non-scratched area at 10 cycles. The byproduct appears to be heaped up at the scratched area.

In the basecoat/topcoat sample coupons, we can see a thin layer developing on the film surface. This layer gets much thinner at 20 cycles, and has disappeared at 30 cycles. At that point, a corrosion byproduct is seen to be covering the film. In the scratched area, we also observe a thin layer at 10 cycles, and as well, a corrosion byproduct covering the scratched area at 30 cycles.

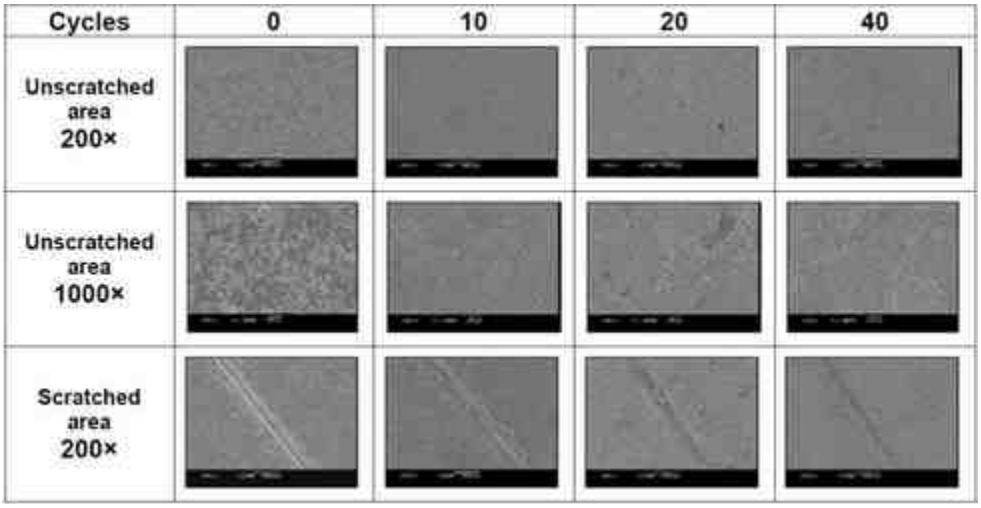

Figure 3 - SEM observation results (basecoat only).

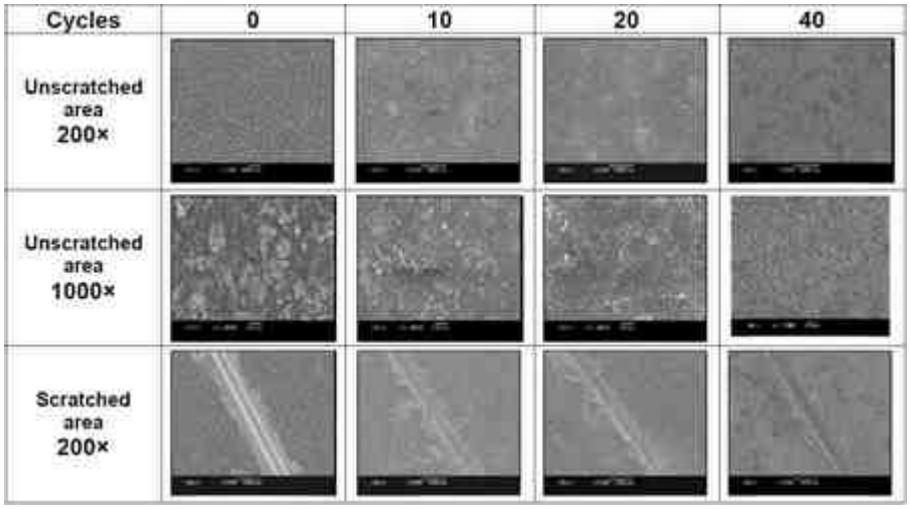

Figure 4 - SEM observation results (both basecoat and topcoat).

Based on this corrosion protection evaluation, the basecoat-only samples demonstrated that zinc and aluminum in the film dissolved and reacted with elements in the atmosphere, generating a corrosion byproduct. On the other hand, when both the basecoat and topcoat were used, at the beginning stage of corrosion, elements from the topcoat formed some kind of layer which covered the basecoat.

SEM-EDS quantitative / qualitative analysis

Tables 2 and 3 show the results of the SEM-EDS quantitative/qualitative analysis of the normal areas described above to verify the transition of each component as the film corrodes. The magnification is 200×.

When only the basecoat is applied (Table 2), silica and aluminum decreased, while chlorine, oxygen and zinc increased at 10 cycles. Accordingly, we see that corrosion byproducts are created from chlorine, oxygen and zinc at the beginning of the corrosion process. At 20 cycles, zinc and chlorine decreased from the levels measured at 10 cycles, while aluminum and oxygen increased. This indicates that a byproduct containing aluminum and oxygen is increasing in volume between 10 and 20 cycles.

Furthermore, chlorine increased again between 20 and 40 cycles, which proves that the formation of the corrosion byproduct changes over time. These changes match the changes seen in the SEM observations (Fig. 3). It appears that corrosion byproducts are thin when there is more chlorine, while they break up and become coarse when there is less chlorine present.

Table 2 - SEM-EDS quantitative / qualitative results (basecoat applied to normal area)(wt%).

Cycles	0	10	20	30	40
Zn	54.8	57.8	49.5	51.6	51.1
Al	23.8	4.2	10.4	8.5	7.0
Si	7.7	0.9	1.6	1.2	2.1
Fe	2.0	2.5	1.1	2.5	2.4
O	8.4	20.3	29.7	27.7	26.3
Cl	0.0	12.2	4.4	5.8	8.6
C	3.2	2.2	3.5	2.6	2.5

Table 3 - SEM-EDS quantitative / qualitative results (basecoat and topcoat applied to normal area)(wt%).

Cycles	0	10	20	30	40
Zn	32.2	51.8	52.4	51.0	48.1
Al	13.1	11.6	11.5	8.0	9.6
Si	21.0	11.0	9.1	4.4	4.1
Fe	2.1	2.8	2.4	2.6	2.4
O	20.8	18.0	19.5	22.6	28.4
Cl	0.0	1.1	1.6	8.3	4.32
C	10.8	3.7	3.7	3.1	3.2

In the sample coupons that received both the basecoat and topcoat (Table 3), silica and carbon decreased and zinc increased at 10 cycles. Silica and carbon are components included in the topcoat. Therefore, we believe that the topcoat is reacting with zinc dissolved from the basecoat, generating a layer that was seen in the SEM observations (Fig. 4).

Tables 4 and 5 show the results of the SEM-EDS quantitative/qualitative analysis of scratched areas (200×) described in the previous section.

Table 4 - SEM-EDS quantitative / qualitative results (basecoat only applied to scratched area) (wt%).

Cycles	0	10	20	30	40
Zn	51.2	56.6	51.8	50.3	52.0
Al	22.1	4.1	8.6	9.3	6.8
Si	7.2	1.4	1.5	1.5	2.9
Fe	9.3	2.6	2.2	3.1	3.5
O	7.4	22.0	27.5	28.4	24.2
Cl	0.0	8.2	5.4	4.3	7.8
C	2.8	5.1	3.2	3.1	2.8

Table 5 - SEM-EDS quantitative / qualitative results (basecoat and topcoat applied to scratched area) (wt%).

Cycles	0	10	20	30	40
Zn	32.3	52.4	54.7	54.5	49.8
Al	13.3	9.5	9.3	6.8	9.3
Si	19.5	12.3	9.2	7.7	2.9
Fe	6.8	3.0	3.1	2.6	2.2
O	18.7	18.9	18.9	20.6	27.5
Cl	0.0	0.8	1.83	3.9	5.5
C	9.31	3.2	3.0	3.9	2.8

The transition of each component in the scratched area is the same as the transition observed in the normal area. Iron significantly decreased at 10 cycles despite the fact that there was a large amount of iron present prior to the evaluation (*i.e.*, at 0 cycles). This also proves that the scratched area was well covered at 10 cycles.

SEM-EDS mapping analysis

Figures 5 and 6 show the results of the SEM-EDS mapping analysis study to determine the distribution of corrosion byproducts at the scratched areas (200×).

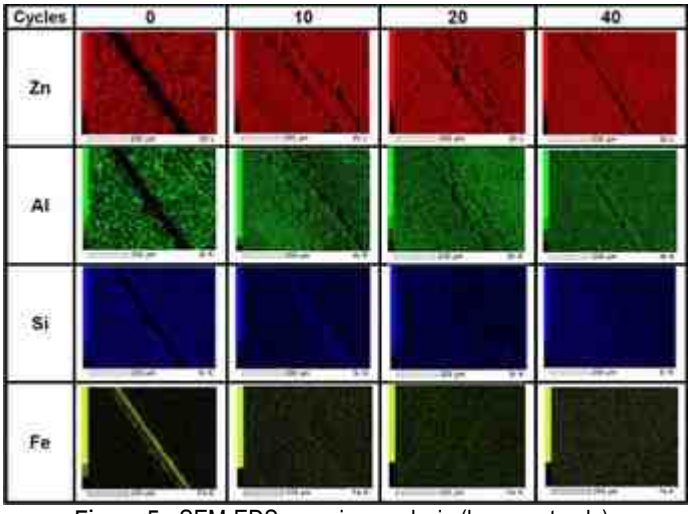

Figure 5 - SEM-EDS mapping analysis (basecoat only).

In the samples that received the basecoat only (Fig. 5), there was no iron detected in the scratched area at 10 cycles. Moreover, we can clearly verify that zinc, aluminum and silica cover over the scratched area. It is also evident in the silicon mapping at 10 cycles that silica is concentrated around the scratched area.

Table 6 shows the SEM-EDS point analysis results of the scratched area at 10 cycles. In the point analysis of the scratched area, we see that the silica and zinc increased. There was byproduct build-up in the scratched area comprised of silica and zinc dissolved from the basecoat, and we believe that the silica from the basecoat greatly contributed to preventing the scratched area from being corroded.

Table 6 - Scratched area analysis; results at 10 cycles.

	Unscratched area	Scratched area (Face side)	Scratched area (Point)
Zn	57.8	56.6	60.0
Al	4.2	4.1	2.66
Si	0.9	1.4	5.4
Fe	2.5	2.6	4.0
O	20.3	22.0	21.9
Cl	12.2	8.2	3.7
C	2.2	5.1	2.3

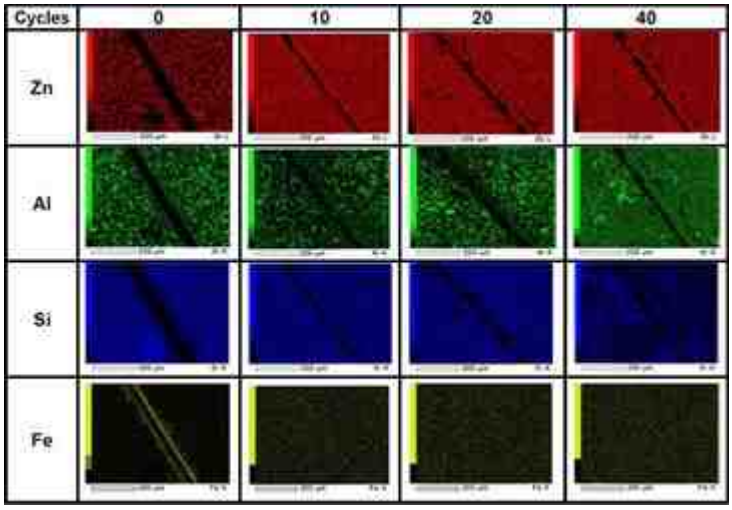

Figure 6 - SEM-EDS mapping analysis (both basecoat and topcoat).

When a sample was processed with both a basecoat and topcoat (Fig. 6), no iron was detected from the scratched area at 10 cycles, similar to the samples processed with the basecoat only. As can be seen from the mapping analysis, at 10 and 20 cycles, the scratched area was covered by both zinc and silica, and aluminum was barely detected. In addition, as zinc was detected over the entire area at 10 cycles, some kind of layer was formed from the zinc and silica from the topcoat. As the component distribution at 30 cycles is very similar to that of the basecoat-only sample, we presume that the corrosion protection mechanism from the topcoat was completed after 30 cycles, and that corrosion would proceed in the same manner as the samples processed with the basecoat only.

Polarization curve analysis

Figures 7 and 8 show the results of the polarization curve measurements to determine the change in surface dissolution in the corrosion test.

According to Fig. 7, a basecoat-only sample progressed and upon reaching 10 cycles in the corrosion protection evaluation, the normal electrode potential of the film was -0.943 V_{SCE}. It is shifted by 0.158 V to the anodic (plus) side as compared to -1.101 V_{SCE} at the beginning of the evaluation (*i.e.,* at 0 cycles). This value is also more noble by 0.048 V than zinc as the standard electrode potential for this type of zinc is -0.988 V_{SCE}. Moreover, the corrosion current density decreased from 5.0×10^{-5} to 5.0×10^{-7} A/cm^2, and there was no corrosion (dissolution) area found on the anodic side of the polarization curve. Therefore, we believe that the corrosion byproduct was present in a passive form, and dissolution of the film (corrosion) was prevented as it was covered with the corrosion byproduct.

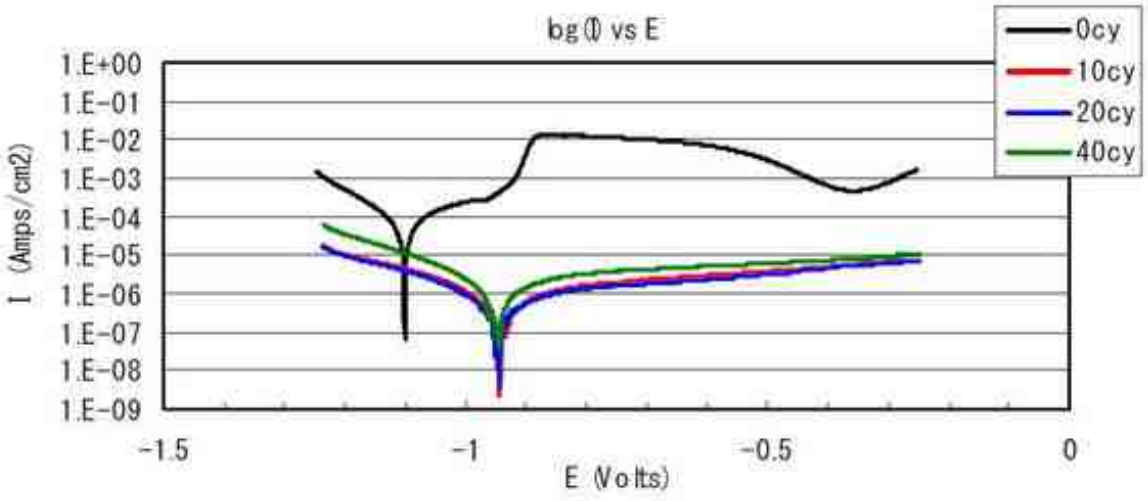

Figure 7 - Polarization curve change in corrosion resistance evaluation (basecoat only).

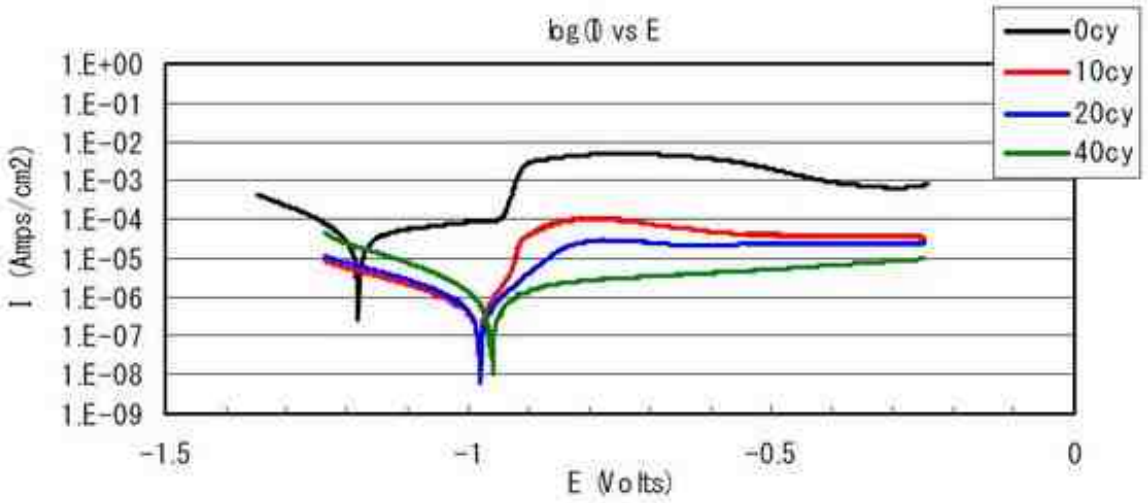

Figure 8 - Polarization curve change in corrosion resistance evaluation (both basecoat and topcoat).

According to Fig. 8, as the corrosion test progressed, the normal electrode potential of the basecoat/topcoat sample shifted to the anodic side and the corrosion current density greatly decreased in the same way as on the basecoat-only sample.

One of the differences from the basecoat-only samples is that there was a corrosion (dissolution) area at 10 and 20 cycles on the anodic side of the polarization curve. Because of this, when the basecoat/topcoat coupons were evaluated, the layer observed at 10 cycles appeared in a weak passivation state as compared to the corrosion byproduct generated in the basecoat-only samples. Therefore, we presume that this layer is made of easily soluble elements.

Tables 7 and 8 show the open-circuit potential measurement results of each test sample. Also shown are the normal electrode potential and the shift of the open-circuit potential away from the normal electrode potential as measured on the test samples.

In general, we can deduce the ratio between oxidants and reductants based on the shift of the open-circuit potential away from the normal electrode potential. The reductants increase when the open-circuit potential shifts to the cathodic (minus) side, and the oxidants increase when the shift is to the anodic (plus) side.

Table 7 - Normal electrode potential and open-circuit potential comparison (basecoat only).

Cycles	0	10	20	40
Normal electrode potential, V_{SCE}	-1.101	-0.943	-0.945	-0.947
Open-circuit potential, V_{SCE}	-1.001	-0.636	-0.636	-0.480
Shift, V	+0.100	+0.307	+0.309	+0.467

In basecoat-only samples (Table 7), we observe about a +0.3 V potential shift, and this confirms that oxidants such as zinc ions (Zn^{+2}) increased at 10 and 20 cycles. Based on this, it appears that corrosion products contain both passivate materials such as zinc oxide (ZnO) and zinc hydroxide ($Zn(OH)_2$) , and oxidants such as zinc ions (Zn^{+2}) and a zinc complex, mixed together. Furthermore, at 40 cycles, when red rust occurs in the scratched area, the potential was shifted to +0.467 V_{SCE}, and oxidants increased. In light of this, we conclude that passivation materials significantly improve corrosion protection.

Table 8 - Normal electrode potential and open-circuit potential comparison (both basecoat and topcoat).

Cycles	0	10	20	40
Normal electrode potential, V_{SCE}	-1.181	-0.981	-0.980	-0.960
Open-circuit potential, V_{SCE}	-1.012	-0.965	-0.933	-0.542
Shift, V	+0.169	+0.017	+0.047	+0.417

When the topcoat is applied (Table 8), the potential is slightly shifted and the oxidants decreased at 10 and 20 cycles. Based on this, we can deduce that the layer formed at 10 and 20 cycles is very close to a passivate-type material, and this formation is an important factor that increases the corrosion protection obtained with the topcoat process.

Summary and conclusions

In our study of silica-type zinc flake coatings, we evaluated the change in the surface condition over time in corrosion testing in order to determine the corrosion protection mechanism. Based on the results, we offer the following conclusions concerning the corrosion protection mechanism:

- Corrosion byproducts (such as $Zn(OH)_2$, Zn_2SiO_4, $ZnCl_2$, ZnO and Zn complexes) are developed when the basecoat is exposed to a corrosive environment and elements dissolved from the basecoat like zinc, aluminum and silicon react with components in the atmosphere such as oxygen gas, chlorides and hydroxides.

- Typical passivation materials in the corrosion byproducts such as $Zn(OH)_2$, ZnO and Zn_2SiO_4 cover the surface of the film, and these covered films demonstrate excellent corrosion resistance as dissolution of the film is prevented.

- A layer is formed between silica, a component of the topcoat, and zinc dissolved from the basecoat film. This layer exhibits superb corrosion protection characteristics as it is very close to a passivation state.

- At scratched areas, silica, a component included in either the basecoat or topcoat, reacts with zinc dissolved in the sacrificial corrosion protection mechanism and it accumulates over the scratch areas, protecting these areas.

Film protection with corrosion byproducts is very important when we want to have protective films with the main objective being sacrificial corrosion protection through film dissolution. In this regard, the film analyses conducted this time during our corrosion studies were very useful.

In the future, we wish to further analyze not only the behavior and components of corrosion byproducts but also their formation mechanism.

References

1. M. Iijima, "High Corrosion Resistance Mechanism of Chrome-Free Zinc-Rich Paint," in *Proc. SUR/FIN 2008, Indianapolis, IN*, NASF, Washington, DC, 2008; p. 345-355.
2. *Manual for Basic Electrochemical Measurements, Short Course*, Electrochemical Society, Pennington, NJ, 2006.

About the authors

Masayuki "Mark" Iijima is a corrosion specialist in the Engineering Department at Yuken Industry in Japan. In his work at Yuken, which is known for its surface treatment processes including plating brighteners and corrosion protection chemicals such as trivalent chromium, he enabled the company to establish a high performance corrosion-resistant coating based on accumulated knowledge and technologies. Before moving on to a new position, Mark was in charge of the zinc-flake coating development since the beginning of this project, assiduously researching the functionality of zinc-rich paint.

Masayuki "Masa" Tsujimoto started working for Yuken Industry in 2003 as an R&D engineer. For a period of five years up to 2008, Masa was initially involved in the development of binders for ceramic molding. During this period, he developed several water-based binders as his focus was on tape film formation employing the Doctor Blade method. Based on this experience in developing binders, Masa was selected in September 2008 to work with the corrosion protection coating development group. He has been a key member of the chromium-free zinc-flake coating project since then, with a particular focus on topcoat development and material improvements.